

# Resolving the Source Populations that Contribute to the X-ray Background: The 2 Ms Chandra Deep Field-North Survey

D. M. ALEXANDER, F. E. BAUER, W. N. BRANDT, G. P. GARMIRE,  
A. E. HORNSCHEMEIER, D. P. SCHNEIDER, AND C. VIGNALI

Department of Astronomy & Astrophysics, 525 Davey Lab, The Pennsylvania State University, University Park, PA 16802.

Received date will be inserted by the editor; accepted date will be inserted by the editor

**Abstract.** With  $\approx 2$  Ms of exposure, the Chandra Deep Field-North (CDF-N) survey provides the deepest view of the Universe in the 0.5–8.0 keV band. Five hundred and three (503) X-ray sources are detected down to on-axis 0.5–2.0 keV and 2–8 keV flux limits of  $\approx 1.5 \times 10^{-17}$  erg cm $^{-2}$  s $^{-1}$  and  $\approx 1.0 \times 10^{-16}$  erg cm $^{-2}$  s $^{-1}$ , respectively. These flux limits correspond to  $L_{0.5-8.0 \text{ keV}} \approx 3 \times 10^{41}$  erg s $^{-1}$  at  $z = 1$  and  $L_{0.5-8.0 \text{ keV}} \approx 2 \times 10^{43}$  erg s $^{-1}$  at  $z = 6$ ; thus this survey is sensitive enough to detect starburst galaxies out to moderate redshift and Seyfert galaxies out to high redshift. We present the X-ray observations, describe the broad diversity of X-ray selected sources, and review the prospects for deeper exposures.

**Key words:** surveys — cosmology — X-rays: active galaxies — X-rays: galaxies

## 1. Introduction

One of the driving goals behind the construction of the *Chandra X-ray Observatory* (hereafter *Chandra*; Weisskopf et al. 2000) was to perform the deepest possible X-ray studies of the Universe. Great advances in this direction have been made with the completion of two  $\approx 1$  Ms surveys [the Chandra Deep Field-North (CDF-N); Brandt et al. 2001a, and the Chandra Deep Field-South (CDF-S); Giacconi et al. 2002]. These ultra-deep *Chandra* surveys resolve the bulk of the 0.5–8.0 keV background, providing the deepest views of the Universe in this band (e.g., Campana et al. 2001; Cowie et al. 2002) and uncovering a broad variety of source populations (see Brandt et al. 2002 for a review).

The CDF-N was awarded a second  $\approx 1$  Ms of *Chandra* exposure in Cycle 3. Here we provide a brief overview of the 2 Ms CDF-N survey and review the prospects for deeper *Chandra* exposures.  $H_0 = 65 \text{ km s}^{-1} \text{ Mpc}^{-1}$ ,  $\Omega_M = \frac{1}{3}$ , and  $\Omega_\Lambda = \frac{2}{3}$  are adopted throughout.

## 2. Observations and Basic Source Properties

The CDF-N observations were obtained with ACIS-I (the imaging array of the Advanced CCD Imaging Spectrometer; Garmire et al. 2002). The 20 observations that comprise the full dataset were taken over a 27 month period; the total exposure time is 1.945 Ms. Each observation was centred close to

the Hubble Deep Field-North (HDF-N; Williams et al. 1996); the total area of the combined observations is  $\approx 460 \text{ arcmin}^2$ . The X-ray data processing was similar to that described in Brandt et al. (2001a) for the 1 Ms *Chandra* exposure.

Five hundred and three (503) X-ray sources are detected with a WAVDETECT false-positive probability threshold of  $10^{-7}$  down to on-axis 0.5–2.0 keV (soft-band) and 2–8 keV (hard-band) flux limits of  $\approx 1.5 \times 10^{-17}$  erg cm $^{-2}$  s $^{-1}$  and  $\approx 1.0 \times 10^{-16}$  erg cm $^{-2}$  s $^{-1}$ , respectively.<sup>1</sup> The adaptively smoothed 0.5–8.0 keV (full-band) 2 Ms *Chandra* image is shown in Figure 1. The  $< 1''$  positional uncertainty for the majority of the X-ray sources allows for accurate cross-correlation to multi-wavelength counterparts.

The range of optical magnitudes for the 503 X-ray detected sources is huge, spanning  $I \approx 13-26$  (note that  $\approx 10\%$  of the sources are optically blank). Two hundred and twenty-four (224) of the sources have redshifts in the literature (e.g., Cohen et al. 2000; Barger et al. 2002), corresponding to  $\approx 45\%$  of the entire sample (see Figure 2). Broad-line AGNs (BLAGNs) are detected out to high redshift (the  $z = 5.186$  AGN is the highest-redshift X-ray selected source known; Barger et al. 2002). Higher redshift AGNs may be detected; however, since Lyman- $\alpha$  leaves the  $I$ -band at  $z \gtrsim 6$ , many will be optically blank (see Alexander et al. 2001 for basic constraints). On average, the  $I < 23$  non-BLAGN sources follow the redshift track expected for an  $L_*$  galaxy (pre-

<sup>1</sup> We searched for X-ray sources in the full, soft, and hard X-ray bands in addition to four sub bands (0.5–1, 1–2, 2–4, and 4–8 keV).

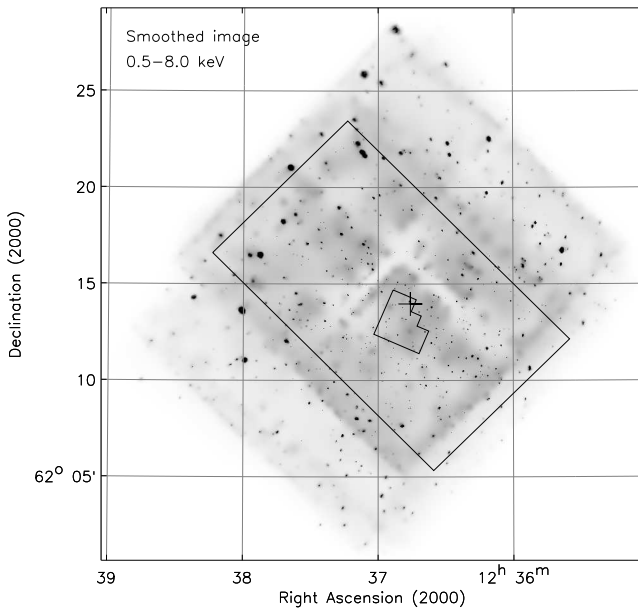


**Fig. 1.** Full-band adaptively smoothed ( $2.5\sigma$ ) image of the CDF-N. Much of the apparent diffuse emission is instrumental background, and the light grooves running through the images correspond to the CCD gaps. The source sizes change across the field due to the spatial dependence of the PSF. The small polygon indicates the HDF-N, the large rectangle indicates the GOODS area, and the cross indicates the average aim point, weighted by exposure time.

sumably the host galaxy dominates the optical emission); the statistics are poor for the  $I = 23\text{--}24$  sources.

Very few  $I \geq 24$  X-ray sources have redshift constraints. However, assuming that they follow the same trend as found for the  $I < 23$  sources, they are likely to lie at  $z \approx 1\text{--}3$  on average (see Alexander et al. 2001 for further discussion). Since these optically faint X-ray sources could account for  $\approx 50\%$  of the AGNs detected in deep *Chandra* surveys (e.g., Alexander et al. 2002c), determining their redshifts will be crucial for AGN studies. Until the advent of 30 metre-class telescopes and *NGST*, photometric redshifts will probably be the most practical method of redshift determination for the majority of these sources. The deep *HST* and ground-based observations obtained as part of the Great Observatories Origins Survey (GOODS) should make this possible for many of the X-ray sources in the CDF-N and CDF-S surveys.<sup>2</sup>

### 3. The Diversity of X-ray Selected Sources

A broad variety of source populations is detected in deep *Chandra* surveys. Here we investigate the diversity of the X-ray selected sources by focusing on the 21.5 arcmin<sup>2</sup> region covered by the deep 15  $\mu\text{m}$  ISOCAM observations of Aussel et al. (1999). In addition to the ISOCAM observations, this region contains the most sensitive X-ray and optical observations (i.e., the HDF-N; Williams et al. 1996). The  $I$ -band

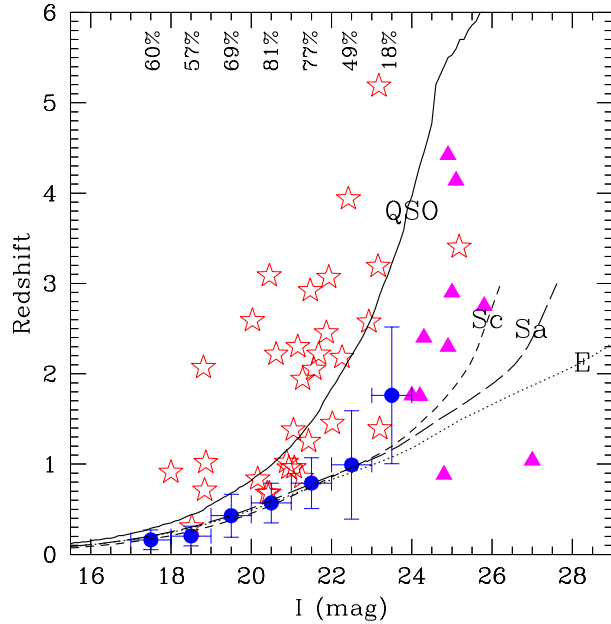


**Fig. 2.** Redshift versus  $I$ -band magnitude for the X-ray sources with known redshifts. The percentages shown at the top correspond to the fraction of  $I = 17\text{--}24$  sources with redshifts. The filled circles indicate the mean redshifts for the non-BLAGN sources and the open stars show the redshifts for the BLAGNs. The filled triangles show individual redshifts for the few  $I \geq 24$  sources with constraints. The curves show the redshift tracks for  $L_*$  galaxies and an  $M_I = -23$  BLAGN (see Alexander et al. 2001 for more details).

magnitude versus full-band flux of the 72 X-ray sources detected in this region is shown in Figure 3.

#### 3.1. AGNs

Following Alexander et al. (2002a) we identify AGNs as those sources with a “Q” (i.e., BLAGN) optical spectral classification from Cohen et al. (2000),  $L_{0.5\text{--}8.0 \text{ keV}} > 3 \times 10^{42} \text{ erg s}^{-1}$ , or a flat effective X-ray spectral slope (i.e.,  $\Gamma < 1.0$ , an indicator of obscured AGN activity).<sup>3</sup> Clearly there can be AGN-dominated sources not selected by these conservative criteria; however, the sources classified here as AGNs should be secure. The AGNs generally fall along the AGN locus defined by Maccacaro et al. (1988) from *Einstein* observations, even though they are  $\approx 4$  orders of magnitude fainter.

A broad variety of AGNs is found. Very luminous AGNs (i.e.,  $L_{0.5\text{--}8.0 \text{ keV}} > 10^{44} \text{ erg s}^{-1}$ ) such as QSOs and obscured QSOs are detected: the former are quite numerous (many of the BLAGNs in Figure 2 are QSOs), while many of the latter may be optically faint and difficult to identify (e.g., the  $I = 25.8$  obscured QSO in the HDF-N; Brandt et al. 2001b). Moderately luminous AGNs such as Seyfert galaxies are detected out to high redshift. The highest redshift Seyfert galaxy identified to date is a  $z = 4.424$  AGN located close to the HDF-N (Waddington et al. 1999; Brandt et al. 2001b).

<sup>3</sup> All X-ray luminosities are calculated in the rest frame conservatively assuming  $\Gamma = 2.0$  and no intrinsic or Galactic absorption.

<sup>2</sup> See <http://www.stsci.edu/science/goods/> for details on GOODS.

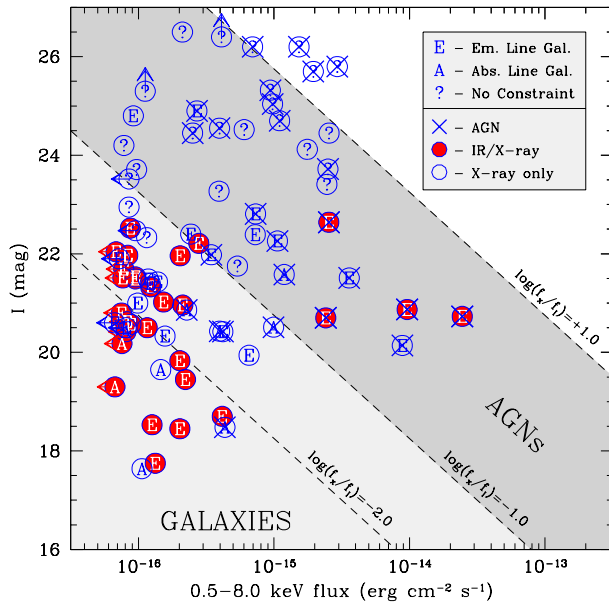


**Fig. 3.**  $I$ -band magnitude versus full-band flux for the 72 X-ray sources detected in the ISOCAM region. The diagonal lines indicate constant flux ratios. The shaded regions show the approximate flux ratios of the AGN-dominated sources and galaxies (both starbursts and normal galaxies). The classifications of the X-ray sources are indicated as shown in the key.

This source has  $L_{0.5-8.0 \text{ keV}} \approx 2 \times 10^{43} \text{ erg s}^{-1}$ ; see Vignali et al. (2002 and this volume) for X-ray spectral analysis of the three  $z > 4$  AGNs in the CDF-N. However, the most commonly detected AGNs are moderate-to-low luminosity sources at  $z \lesssim 1$ . These AGNs show a variety of characteristics, including sources with emission-line dominated spectra and sources with absorption-line dominated spectra (e.g., Hornschemeier et al. 2001; Brandt et al. 2001b).

X-ray spectral analysis of the X-ray brightest AGNs are presented in Bauer et al. (this volume). Amongst other things they report a diversity in the X-ray spectral properties of the AGNs and show that the classical view of BLAGNs having unobscured X-ray continua may not hold at the X-ray fluxes of this survey.

### 3.2. Starbursts and normal galaxies

A large number of apparently normal galaxies are detected at faint X-ray fluxes (i.e., full-band fluxes  $< 5 \times 10^{-16} \text{ erg cm}^{-2} \text{ s}^{-1}$ ; Hornschemeier et al. 2001). A good indication of the nature of these sources is found by cross-correlating them with  $15 \mu\text{m}$  ISOCAM sources. In the 2 Ms dataset we find that 29 of the 40 ( $\approx 73\%$ ) ISOCAM galaxies in the complete ( $f_{15\mu\text{m}} \geq 100 \mu\text{Jy}$ ) sample of Aussel et al. (in preparation) have X-ray counterparts.<sup>4</sup> The majority ( $\approx 80\%$ )

of the X-ray detected  $15 \mu\text{m}$  sources appear to be emission-line galaxies (ELGs) without apparent AGNs; by comparison, AGNs and absorption-line galaxies comprise  $\approx 15\%$  and  $\approx 5\%$ , respectively. Of course it is possible that some of the X-ray detected ELGs contain an AGN not identified by our conservative criteria; however, their stacked-average X-ray spectral slope ( $\Gamma \approx 2.0$ ) suggests that few obscured AGNs are likely to be present. The most likely scenario is that these sources are predominantly luminous infrared starburst galaxies (e.g., Alexander et al. 2002a), a conclusion entirely consistent with analyses of the faint  $15 \mu\text{m}$  ISOCAM source population (e.g., Chary & Elbaz 2001).

The range of redshifts and X-ray luminosities for these sources is broad ( $z = 0.078-1.275$  and  $L_{0.5-2.0 \text{ keV}} = 10^{39}-10^{42} \text{ erg s}^{-1}$ ). While the X-ray emission from the low-redshift, low-luminosity sources could be produced by a single ultra-luminous X-ray source (e.g., Hornschemeier et al. 2002b), the majority of these sources have X-ray luminosities between those of M 82 and NGC 3256, implying moderate-to-luminous star-formation activity (i.e.,  $\approx 10-100 M_{\odot}$ ). The two most luminous sources have X-ray luminosities  $\approx 3$  times greater than that of NGC 3256, the most X-ray luminous starburst galaxy known. The steep X-ray spectral slopes of these two sources ( $\Gamma > 1.5$  and  $\Gamma > 1.8$ ) suggests that neither are obscured AGNs.

Most of the X-ray detected ELGs are also detected at radio wavelengths (Bauer et al. 2002), providing additional support for the starburst galaxy hypothesis. Indeed, the X-ray and radio luminosities of these sources are correlated and agree with those found for local starburst galaxies, suggesting that the X-ray emission can be used directly as a star-formation indicator (see also Ranalli, this volume).

## 4. Prospects for Deeper Chandra Exposures

In examining the prospects for deeper *Chandra* exposures we first review the observations within the extremely sensitive  $5.3 \text{ arcmin}^2$  HDF-N region (e.g., Williams et al. 1996). All of the 20 X-ray sources in the HDF-N have optical counterparts down to  $I \approx 28$  and all have spectroscopic or photometric redshifts (see Figure 4); further sources can be found by matching lower-significance *Chandra* sources to optically bright galaxies (e.g., Figure 5 of Brandt et al. 2002).

The density of X-ray sources in the HDF-N is  $\approx 12,000 \text{ deg}^{-2}$  and  $\approx 6,000 \text{ deg}^{-2}$  for the soft and hard bands, respectively. These are the highest source densities reported for a blank-field X-ray survey, although they are low when compared to the optical source density of the HDF-N ( $\approx 2 \times 10^6 \text{ deg}^{-2}$ ; e.g., Williams et al. 1996). Since the (conservative) source confusion limit for on-axis *Chandra* observations is  $\approx 80,000 \text{ deg}^{-2}$ , source confusion is unlikely to start becoming a problem until significantly fainter X-ray flux limits are reached (the source confusion limit is calculated assuming 20 beams per source and a 1.5 arcsec 95% encircled energy radius). The average  $\approx 2 \text{ Ms}$  *Chandra* background is  $\approx 0.4 \text{ counts pixel}^{-1}$  in the  $0.5-8.0 \text{ keV}$  band, suggesting that *Chandra* should remain close to photon limited for exposures up to  $\approx 5 \text{ Ms}$ , on axis; the situation is even more

<sup>4</sup> The matching was performed to sources detected in any of the seven X-ray bands; 26 sources are detected in at least one of the three main bands.

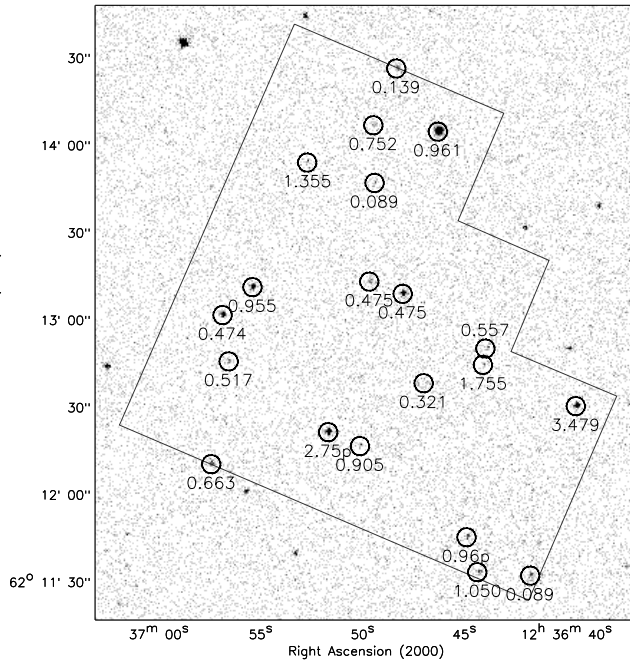


**Fig. 4.** Full-band *Chandra* image of the HDF-N and its immediate environs. The polygon indicates the HDF-N, and the circles indicate the X-ray detected sources. Source redshifts are shown above or below each source (p indicates a photometric redshift). See <http://www.astro.psu.edu/users/niel/hdf/hdf-chandra.html> for a movie of the HDF-N for  $\approx 25$ –1945 ks *Chandra* exposures.

favourable in the X-ray bands with lower background rates (e.g., the 0.5–2.0 keV band). Clearly deeper *Chandra* exposures can reach significantly deeper flux limits efficiently and be free of source confusion.

Several analyses have provided *direct* evidence that deeper *Chandra* exposures will detect a significantly larger number of sources. For instance, X-ray stacking analyses of normal galaxies have suggested that  $\approx L_*$  galaxies at  $z < 1.5$  should be detected in significant numbers with 0.5–2.0 keV fluxes of  $\approx (3\text{--}6) \times 10^{-18}$  erg cm $^{-2}$  s $^{-1}$  (e.g., Hornschemeier et al. 2002a).<sup>5</sup> These results are bolstered by X-ray fluctuation analyses and model simulations which have implied a rise in the number counts around 0.5–2.0 keV fluxes of  $\approx 7 \times 10^{-18}$  erg cm $^{-2}$  s $^{-1}$  (Miyaji & Griffiths 2002; Ptak et al. 2001). A  $\approx 5$  Ms *Chandra* survey can achieve on axis 0.5–2.0 keV fluxes of  $\approx 6 \times 10^{-18}$  erg cm $^{-2}$  s $^{-1}$ .

A 5–10 Ms *Chandra* exposure can reach the flux limits being discussed for the next generation of X-ray observatories such as *XEUS* (not to be launched for 10–15 years). Although the prime scientific focus of *XEUS* is X-ray spectral analysis, an ultra-deep *Chandra* survey can explore the likely source populations to be detected in deep *XEUS* surveys, and provide firm constraints on the X-ray source density.

<sup>5</sup> Stacking analyses of Lyman-break galaxies and VROs/EROs have also suggested that the average source should be detectable at these fluxes (e.g., Brandt et al. 2001c; Alexander et al. 2002b).

**Acknowledgements.** This work has been largely possible due to the financial support of NASA grants NAS 8-38252 and NAS 8-01128, the NSF CAREER award AST-9983783, and CXC grant G02-3187A.

## References

Alexander, D. M., Brandt, W.N., Hornschemeier, A.E., Garmire, G.P., Schneider, D.P., Bauer, F.E., & Griffiths, R.E.: 2001, AJ, 122, 2156

Alexander, D. M., Aussel, H., Bauer, F. E., Brandt, W. N., Hornschemeier, A. E., Vignali, C., Garmire, G. P., & Schneider, D. P.: 2002a, ApJ, 568, L85

Alexander, D. M., Vignali, C., Bauer, F.E., Brandt, W.N., Hornschemeier, A.E., Garmire, G.P., & Schneider, D.P.: 2002b, AJ, 123, 1149

Alexander, D. M., Bauer, F.E., Brandt, W.N., Hornschemeier, A.E., Vignali, C., Garmire, G.P., & Schneider, D.P.: 2002c, in *New Visions of the X-ray Universe*, in press (astro-ph/0202044)

Aussel, H., Cesarsky, C. J., Elbaz, D., & Starck, J. L.: 1999, A&A, 342, 313

Barger, A. J., et al.: 2002, AJ, 124, 1839

Bauer, F. E., Alexander, D. M., Brandt, W. N., Hornschemeier, A. E., Vignali, C., Garmire, G. P., & Schneider, D. P.: 2002, AJ, 124, 2351

Brandt, W. N., et al.: 2001a, AJ, 122, 2810

Brandt, W. N., et al.: 2001b, AJ, 122, 1

Brandt, W. N., Hornschemeier, A.E., Schneider, D.P., Alexander, D.M., Bauer, F.E., Garmire, G.P., & Vignali, C.: 2001c, ApJ, 558, L5

Brandt, W. N., Alexander, D. M., Bauer, F. E., Hornschemeier, A. E.: 2002, Philos. Trans. R. Soc. London, A, 360, 2057

Campana, S., Moretti, A., Lazzati, D., & Tagliaferri, G.: 2001, ApJ, 560, L19

Chary, R. & Elbaz, D.: 2001, ApJ, 556, 562

Cohen, J. G., Hogg, D.W., Blandford, R., Cowie, L.L., Hu, E., Songaila, A., Shopbell, P., & Richberg, K.: 2000, ApJ, 538, 29

Cowie, L. L., Garmire, G. P., Bautz, M. W., Barger, A. J., Brandt, W. N., & Hornschemeier, A. E.: 2002, ApJ, 566, L5

Garmire, G. P., Bautz, M. W., Ford, P. G., Nousek, J. A., & Ricker, G. R.: 2002, Proc. SPIE, 4851, in press

Giacconi, R. et al.: 2002, ApJS, 139, 369

Hornschemeier, A. E., et al.: 2001, ApJ, 554, 742

Hornschemeier, A. E., Brandt, W. N., Alexander, D. M., Bauer, F. E., Garmire, G. P., Schneider, D. P., Bautz, M. W., & Chartas, G.: 2002a, ApJ, 568, 82

Hornschemeier, A. E., et al.: 2002b, AJ, submitted

Maccacaro, T., Gioia, I. M., Wolter, A., Zamorani, G., & Stocke, J. T.: 1988, ApJ, 326, 680

Miyaji, T. & Griffiths, R. E.: 2002, ApJ, 564, L5

Ptak, A., Griffiths, R., White, N., & Ghosh, P.: 2001, ApJ, 559, L91

Vignali, C., Bauer, F. E., Alexander, D. M., Brandt, W. N., Hornschemeier, A. E., Schneider, D.P., & Garmire, G.P.: 2002, ApJ, 580, L105

Waddington, I., Windhorst, R.A., Cohen, S.H., Partridge, R.B., Spinrad, H., & Stern, D.: 1999, ApJ, 526, L77

Weisskopf, M. C., Tananbaum, H.D., Van Speybroeck, L.P. & O'Dell, S.L.: 2000, Proc. SPIE, 4012, 2

Williams, R.E., et al.: 1996, AJ, 112, 1335